

Localization, Tracking and Following a Moving Target by an RFID Equipped Robot

George Mylonopoulos
School of ECE, AUTH
Thessaloniki, Greece
gmylonop@ece.auth.gr

Aristidis Raptopoulos Chatzistefanou
School of ECE, AUTH
Thessaloniki, Greece
raptopak@ece.auth.gr

Alexandros Filotheou
School of ECE, AUTH
Thessaloniki, Greece
alefilot@auth.gr

Anastasios Tzitzis
School of ECE, AUTH
Thessaloniki, Greece
atzitzis@ece.auth.gr

Stavroula Siachalou
School of ECE, AUTH
Thessaloniki, Greece
ssiachal@ece.auth.gr

Antonis G. Dimitriou
School of ECE, AUTH
Thessaloniki, Greece
antodimi@auth.gr

Abstract—In this paper, we present a prototype algorithm for tracking and following a moving target through RFID technology by a robot. The robot is equipped with two front facing antennas, which collect phase measurements of the tag's modulated signal. We consider a direction-finding algorithm, based on particle filter theory, which exploits the phase-measurements to assign weights to the particles. The proposed track-and-follow robot is successfully tested in a laboratory environment and will be deployed inside a museum.

Index Terms—RFID, Tracking, Localization, Angle of Arrival

I. INTRODUCTION

In this paper, we propose a prototype algorithm that allows a robot to track and follow autonomously a moving target, through RFID technology. The robot is designed in the context of project "CultureID" [1], where an RFID-enabled social robot will be installed inside the Archaeological Museum of Thessaloniki. Among others, the robot will play "games" with younger visitors. In such context, the robot will be able to follow a visitor, who holds an RFID-tag. In general, the track-and-follow problem in robotics is of interest in large warehouses, where mobile robots are required to co-operate with personnel or other robots.

The robot is equipped with two front-facing antennas and a monostatic RFID reader. The angle of arrival can be derived from the measured phase [2]- [7], giving the target's direction relative to the robot's pose. The robot is capable to create a 3D map of the surrounding environment [8], [9] and localize itself in the map at cm accuracy. It can safely navigate autonomously inside the map and dynamically create optimal paths, adjusting its decisions in real-time, depending on the changes of the surrounding environment.

The problem of track-and-follow has been treated in prior-art mainly by deploying solutions, based on vision [10]. RFID

This research has been co-financed by the European Union and Greek national funds through the Operational Program Competitiveness, Entrepreneurship and Innovation, under the call RESEARCH – CREATE – INNOVATE (project code:T2EDK-02000).

has been deployed for the specific problem, where both the target and the robot move in [11]- [12]. In [11] the authors exploit only the measured power from two antennas facing different orientations to estimate the direction of the target. More recently, in [12] the authors propose an algorithm that can track the location of the target based on phase measurements collected along two antennas. The measurements are treated separately per antenna and the unwrapped phase measured per antenna is used as the input to the robot to successfully maintain its distance from the target.

In our case, the problem is somehow different. We do not expect the robot to be able to maintain a constant distance from the target, i) due to the speed-constraint of the robot (the robot will move at a maximum speed of 50cm/s) and ii) due to blocking of the tag around corners in the exhibition area. As a result the following robot is expected to suffer from frequent interruptions of tag-readings. In the treated problem, we aim to identify only the direction of the target, the robot-to-target distance is expected to change frequently, as the visitor will move much faster than the robot and the robot will eventually reach the human and stop at 1m from the target, by deploying its lidar sensor. Taking the above into considerations, we propose a direction-tracking algorithm, exploiting the phase-difference measurement between two antennas which is fed into a particle filter algorithm. Furthermore, we take into account the frequent "loss" of the target to deploy another "discovery" strategy in the initialization of a new particle tracking stage.

II. PROPOSED METHOD

In case of a monostatic RFID reader, equipped with two antennas, as shown in Fig. 1, the angle of arrival of the backscattered RFID signal can be estimated using the measured phase difference between two antennas and is approximated by [2] [4]

$$\theta = \arcsin\left(\frac{\Delta\phi \times \lambda}{4\pi \times L}\right) \quad (1)$$

where λ is the wavelength of the carrier frequency ($f_c = 866.5\text{MHz} \rightarrow \lambda = 0.345\text{m}$) and L is the distance between the two antennas. Equation (1) is less accurate as the tag-to-reader distance decreases. Due to phase-wrapping, the phase measured by the n^{th} antenna is

$$\phi_n^{\text{exp}}(d_n) = \left(\frac{2\pi}{\lambda} 2d_n + \phi_n^0 \right) \bmod 2\pi, \quad n \in [1, N]. \quad (2)$$

where d_n is the distance between the n^{th} antenna and the tag and ϕ_n^0 is a phase-term related to the specific antenna; i.e. accounting for the antenna-to-reader cable's length, the phase-shift of the specific reader-port etc. This term can be measured and extracted from the calculations. Then (2) becomes:

$$\phi_n^{\text{exp}}(d_n) = \left(\frac{2\pi}{\lambda} 2d_n \right) \bmod 2\pi, \quad n \in [1, N]. \quad (3)$$

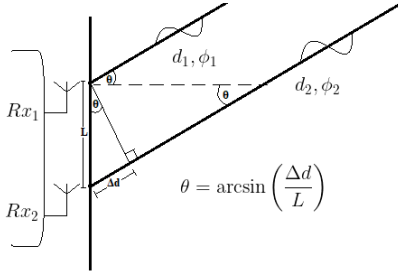


Fig. 1. The geometry of SD-PDOA for two antennas

As the measured phase is wrapped in $[0, 2\pi)$, the actual phase difference between the measured phase from the 1^{st} antenna at $t = i$ and the 2^{nd} antenna at $t = j$ is

$$\Delta\phi_{12} = \phi_1^i - \phi_2^j + 2k\pi \quad (4)$$

$$k = \dots, -1, 0, 1, \dots$$

The number of possible k in (4) depends on the inter-antenna distance L [2] Considering (1) $\frac{\Delta\phi \times \lambda}{4\pi \times L}$ is bound within $[-1, 1]$

$$\Delta\phi_{12} \in \left[-\frac{4\pi \times L}{\lambda}, \frac{4\pi \times L}{\lambda} \right] \quad (5)$$

Assuming $L \leq \lambda/4$, the ambiguity is eliminated. So, it might seem like a good strategy to place the antennas as close as possible. However, the measured phases also suffer from zero-mean Gaussian errors; in the available reader the standard deviation of the phase-error equals 0.1 rad. As the distance between the reader-antennas becomes smaller, the effect of the measurement-error on the estimated-direction increases. The magnitude of this effect grows at the limits of the target area (close to $\pm\pi/2$), due to the non-linearity of the \arcsin function of (1). This effect is demonstrated in Fig. 2 for $L = 0.13\text{m}$. Furthermore, due to the physical dimensions of the available antennas, the two antennas are typically placed at $\lambda/4 \leq L \leq \lambda/2$. Under such conditions, we can identify two angular regions. One ambiguous-free region, around the direction of maximum radiation of the two antennas (around

$\theta = 0$) and another region, where the ambiguity is reduced to two possible values:

$$k = \begin{cases} \{0, -1\}, & \Delta\phi_{12} \geq 0 \\ \{0, +1\}, & \Delta\phi_{12} < 0 \end{cases} \quad (6)$$



Fig. 2. The estimation error with and without noise

In our case, the two antennas are placed in front of the robot with an inter-antenna distance $L = 0.13\text{m}$. By substituting the specific L , the ambiguous estimation described in (6), exists for $\text{abs}(\Delta\phi_{12}) > 2\pi - \frac{4\pi \times L}{\lambda} \approx 1.548$ which represents an estimated angle of arrival of $\pm 19.08^\circ$

Unwrapping the measured phase would eventually disambiguate the possible estimations, but the experimental data are not necessarily dense-enough to do phase-unwrapping. For example, consider the human-carrying-a-tag suddenly turning and being lost from the robot; the measured data would be discontinued and phase-unwrapping impossible.

A. Deployment of Particle Filters

We have deployed Particle-Filter theory, [13]- [17], in order to keep track of the target, as explained below. The particles' prime attribute is their azimuth relative to the robot, but more dimensions could be added describing the target's distance to the reader, its velocity and its acceleration. However the added complexity does not deem necessary, since each new attribute should be accompanied by an appropriate measurement input (i.e. if the RSSI measurement was only distance dependant it could serve as a ranging detection input). Therefore each particle is defined as a direction in $[-\pi/2, \pi/2]$, θ_k , i.e.:

$$\mathbf{x}_k^i = (\theta_k^i), i = 1, \dots, N \quad (7)$$

and k refers to the discrete time-step of each new set of estimations and θ_k^i is the target's angle relative to the robot's pose. As described above, there is an ambiguity free zone $\theta_{\text{tag}} \in (-19^\circ, 19^\circ)$, which is used to initialise the Target Tracking Algorithm (TTA). An initial distribution of

$$\pi_\theta^i(t_0) = \mathbb{N}(0, \sigma_{\text{std}}) \quad (8)$$

produces an approximate first indication of the target's direction, which is then updated with the future pair of estimations. The lack of ambiguity in the central target angular

zone ensures that the total set of particles clusters around the single correct estimation. Given that the target's speed is reasonably limited and its angular displacement between estimations does not exceed an upper threshold, there should be no ambiguity regarding the target's direction, since the particles cluster around the estimation that is developed from the initial distribution. After each new set of estimations that serves as input to the PF, the weight of each particle $\{x_k^i\}_{i=1}^N$ is given by

$$w_k^i = \frac{\pi - \min(\text{divergence}_j)}{\pi}, \quad j \in \{1, 2\} \quad (9)$$

where divergence_j refers to the particles' angular distance from the two measured possible estimations due to the phase ambiguity, defined in (4) and (6). During time step k , the angle of the target is given by the top 30% dominant particles by their weighted sum:

$$\theta_k^{\text{est}} = \frac{\sum_{\text{top 30\%}} w_k^i \theta_k^i}{\sum_{\text{top 30\%}} w_k^i} \quad (10)$$

New particles are created around the top 30% dominant particles of the previous instance, so that the total number of particles becomes N . The distribution of the new particles is given by

$$\pi_{\theta}^i(t_k) = \mathbb{N}(\mu_{\theta_{k-1}^i}, \sigma_{\text{std}}) \quad (11)$$

where $\mu_{\theta_{k-1}^i}$ is the azimuth of each parent particle. The standard deviation is constant for this instance, but it could become a variable depending on the particle's velocity if additional dimensions are added to the particles. It is apparent that the quality of the PF's output is heavily dependant on the previous outputs, since a single bias towards the alternative target direction would lock the TTA on this bearing indefinitely. Therefore, it is important to create a reliability indicator. That indicator depicts the divergence of the particles $\{x_k^i\}_{i=1}^N$ from the pair of estimations for each step. If each particle update falls beneath a certain divergence threshold, it is considered a reliable set of transitions that lead to the final output. Moreover, the data density is expected to drop when the target lies close to the edges of the desired operational angular domain. It is expected that there will be readings outside the desired domain, which can be identified by the expected density drop. If the transition is not reliable, the last reliable output is considered to be true, and the robot is expected to find the target within the ambiguity free zone for the TTA to be initialised again.

In order for such a feature to work a Target Finding Algorithm (TFA) is implemented, where the robot rotates towards the last reliable estimation, until the target lies within the ambiguity free zone. This is achieved with a different initial distribution of the particles

$$\pi_{\theta}^i(t_0) = \mathbb{N}\left(X \frac{\pi}{2}, \sigma_{\text{std}}\right) \quad (12)$$

$$X \in \{-1, 1\}$$

$$\Pr\{X = -1\} = \Pr\{X = 1\} = \frac{1}{2}$$

which implies that since the target is outside the operating angular domain, it will first appear on the side. The TFA can be used for the initialisation of the system, making the robot face the target.

The importance of continuous reliable PF outputs significantly limits the robot's ability to navigate freely in space since the antennas are turning with the robot as it is moving. Thus, the robot's need to perform obstacle avoiding maneuvers can potentially drive the target outside the operating angular domain; especially for tight spaces where sharp turns are necessary. This problem has been solved via the robot's access to the environment's morphology. We have constrained the path-planning algorithm of the robot on a specific network of nodes, which enable the robot of reaching the target everywhere within the map, producing a smooth and natural-like movement. The Node Navigation Algorithm (NNA) takes the reliable TTA estimations while travelling between nodes and makes a new target when it is within a small range from its current goal. The constructed map with the set of nodes is shown in Fig. 3. The latter setting, makes the proposed algorithm robust for application in crowded uncontrolled environments, like the museum.

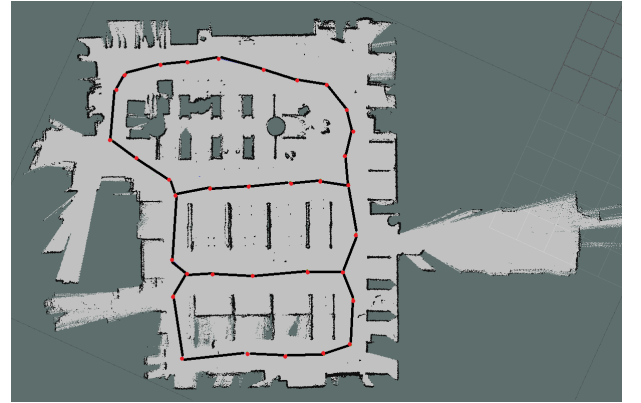


Fig. 3. 2D representation of the environment constructed from the robot, with the necessary nodes to navigate

III. EXPERIMENTS

Numerous experiments were conducted inside a computer-lab; the map is shown in Fig. 3. Initially, the robot was still and the target was moved arbitrarily in front of the robot, within the read-zone. The proposed particle-filter tracker performed remarkably well, in contrast to a brute-force algorithm which considered only the latest measurement. Characteristic results are shown in Figs. 4-5.

During the next experimental phase, the target tag moved freely throughout the lab and the robot, was tasked to follow the tag, applying the proper combination of the TTA and the TFA. In all cases the robot successfully followed the tag, applying the TTA, when the tag was within measurement-range of the robot and then re-discovered the target, applying the TFA, when the target was lost after turning around corners.

This process was successfully tested repeatedly more than 20 times.

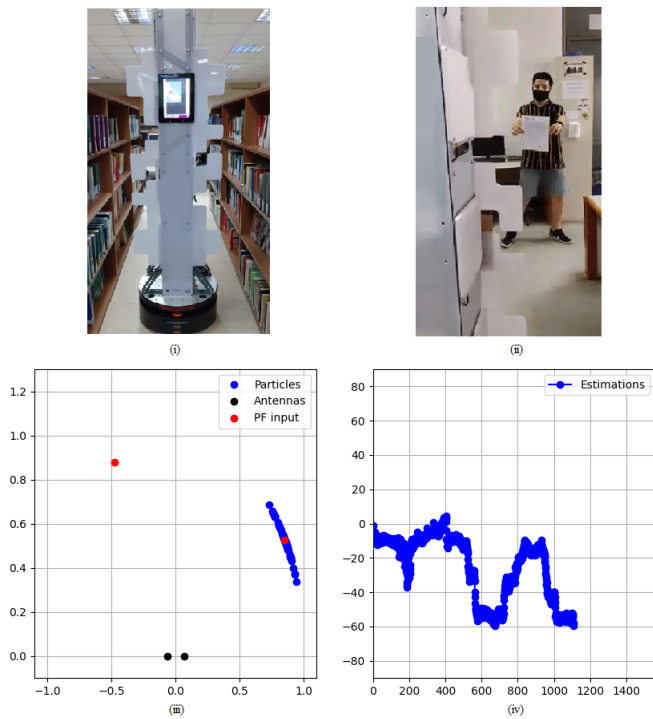


Fig. 4. The robot stationary (i) and during the experiment (ii) with the particles (iii) and the output (iv) during the experiment

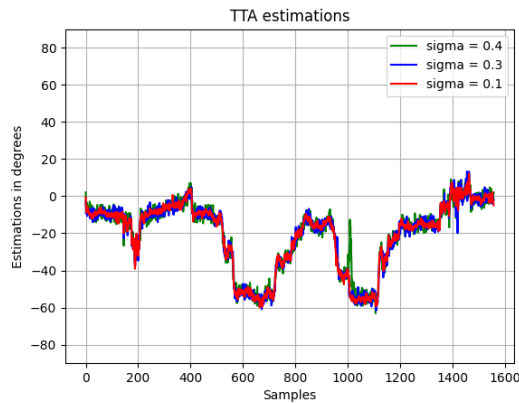


Fig. 5. Experiment No.2: PF output

IV. CONCLUSIONS

After combining well known techniques found in prior-art, a well-structured design is presented that fulfills the desired criteria. The SD-PDOA technique may be subject to ambiguity due to the physical size of the antennas, but Particle-Filtering and proper processing of the extracted estimations may lead to an effective and reliable algorithm that tracks the target's movement relative to the robot. The robot's SLAM abilities

allow for an effective track and follow system to be implemented. Further development is possible, both with hardware extensions (i.e. antennas rotating independently to the robot) or additional algorithms (i.e. target's path reconstruction through Particle-Filtering) that would enable the robot to keep the target within the desired region more effectively and enhance the particles characteristics (i.e. speed and acceleration).

REFERENCES

- [1] CultureID. The Internet of Culture. Embedding RFID Technology in the Museum. Accessed May. 13, 2021 [Online]. Available: <https://cultureid.web.auth.gr>.
- [2] A. G. Dimitriou, S. Siachalou, E. Tsardoulas, L. Petrou, "Robotics Meets RFID for Simultaneous Localization (of Robots and Objects) and Mapping (SLAM) – a Joined Problem," in *Wireless Power Transmission for Sustainable Electronics: COST WiPE-IC1301*, John Wiley and Sons, March 2020. Inc. <https://doi.org/10.1002/9781119578598.ch7>.
- [3] D. Dobkin, *The RF in RFID Passive UHF RFID in Practice*. Imprint of Butterworth-Heinemann Ltd. 313 Washington St. Newton, MA, United States: Newnes, 2007.
- [4] P. V. Nikitin, R. Martinez, S. Ramamurthy, H. Leland, G. Spiess, and K. V. S. Rao, "Phase based spatial identification of uhf rfid tags," in *2010 IEEE International Conference on RFID (IEEE RFID 2010)*, pp. 102–109, IEEE, 2010.
- [5] R. Kronberger, T. Knie, R. Leonardi, U. Dettmar, M. Cremer, and S. Azzuzi, "Uhf rfid localization system based on a phased array antenna," in *2011 IEEE International Symposium on Antennas and Propagation (APSURSI)*, pp. 525–528, IEEE, 2011.
- [6] F. Quitin, V. Govindaraj, X. Zhong and W. P. Tay, "Virtual Multi-Antenna Array for Estimating the Angle-of-Arrival of a RF Transmitter," 2016 IEEE 84th Vehicular Technology Conference (VTC-Fall), 2016, pp. 1–5, doi: 10.1109/VTCFall.2016.7881965.
- [7] Y. Fu, C. Wang, R. Liu, G. Liang, H. Zhang, and S. Ur Rehman, "Moving object localization based on uhf rfid phase and laser clustering," in *Sensors*, 18(3), p. 825, 2018.
- [8] A. Filotheou, E. G. Tsardoulas, A. Dimitriou, A. L. Symeonidis and L. Petrou, "Quantitative and qualitative evaluation of ROS-enabled local and global planners in 2D static environments," *J. Intell. Robot. Syst.*, vol. 98, pp. 567–601, 2020.
- [9] A. Filotheou, E. G. Tsardoulas, A. G. Dimitriou, A. L. Symeonidis and L. Petrou, "Pose selection and feedback methods in tandem combinations of particle filters with scan-matching for 2D mobile robot localisation," *J. Intell. Robot. Syst.*, vol. 100, pp. 925–944, 2020.
- [10] Y. Wu, J. Lim, and M. H. Yang, "Object tracking benchmark," *IEEE Trans. Pattern Anal. Mach. Intell.*, vol. 37, no. 9, pp. 1834–1848, Sep. 2015.
- [11] M. Kim, N. Y. Chong, H. Ahn and W. Yu, "RFID-enabled Target Tracking and Following with a Mobile Robot Using Direction Finding Antennas," *2007 IEEE International Conference on Automation Science and Engineering*, 2007, pp. 1014–1019, doi: 10.1109/COASE.2007.4341763.
- [12] C. Wu, B. Tao, H. Wu, Z. Gong and Z. Yin, "A UHF RFID-Based Dynamic Object Following Method for a Mobile Robot Using Phase Difference Information," in *IEEE Transactions on Instrumentation and Measurement*, vol. 70, pp. 1–11, 2021, Art no. 8003611, doi: 10.1109/TIM.2021.3073712.
- [13] D. Angelova and L. Mihaylova, "Joint target tracking and classification with particle filtering and mixture kalman filtering using kinematic radar information," in *Digital Signal Processing*, 16(2), pp. 180–204, 2006.
- [14] X. L. Hu, T. B. Sch"on, and L. Ljung, "A basic convergence result for particle filtering," in *IFAC Proceedings Volumes*, 40(12), pp. 288–293, 2007.
- [15] A. H. Jazwinski, "Stochastic processes and filtering theory," in *Stochastic Processes and Filtering Theory*, Vol. 64 of Math, Academic Press, New York, 1970.
- [16] G. L. Smith, S. Schmidt, and L. A. McGee, "Application of statistical filter theory to the optimal estimation of position and velocity on board a circumlunar vehicle," in *National Aeronautics and Space Administration*, 1962.
- [17] A. Motroni, A. Buffi, P. Nepa and B. Tellini, "Sensor-Fusion and Tracking Method for Indoor Vehicles With Low-Density UHF-RFID Tags," in *IEEE Transactions on Instrumentation and Measurement*, vol. 70, pp. 1–14, 2021, Art no. 8001314, doi: 10.1109/TIM.2020.3027926.